AMERICAN SOCIETY FOR MICROBIOLOGY | mSphere®

RESEARCH ARTICLE

Eukaryotic Initiation Factor 2α Kinases Regulate Virulence Functions, Stage Conversion, and the Stress Response in *Entamoeba invadens*

Heather A. Walters,[a,b] Brenda H. Welter,[a,b] Harrison C. Moss,[a,b] Martha A. Villano,[a,b] Ronny Orobio-Hurtado,[a,b] William J. Sullivan, Jr.,[c,d] Lesly A. Temesvari[a,b]

[a]Department of Biological Sciences, Clemson University, Clemson, South Carolina, USA
[b]Eukaryotic Pathogens Innovation Center (EPIC), Clemson University, Clemson, South Carolina, USA
[c]Department of Pharmacology and Toxicology, Indiana University School of Medicine Indianapolis, Indiana, USA
[d]Department of Microbiology and Immunology, Indiana University School of Medicine Indianapolis, Indiana, USA

ABSTRACT *Entamoeba histolytica* is a protozoan parasite that causes amoebic dysentery and liver abscess. This pathogen possesses a two-stage life cycle consisting of an environmentally stable cyst and a pathogenic amoeboid trophozoite. Since infection is acquired by ingestion of cysts from contaminated food and water, this parasite is prevalent in underdeveloped countries. A reptilian pathogen, *Entamoeba invadens*, which can encyst in culture, has long served as a surrogate to study stage conversion. In the host, *Entamoeba* species must manage stress, including nutrient deprivation and host immune pressure. In many systems, the stress response is characterized by downregulation of translation, which is initiated by the phosphorylation of eukaryotic initiation factor-2 alpha (eIF2α). In mammalian cells, this phosphorylation is carried out by a family of eIF2α kinases. A canonical eIF2α translational control system exists in *Entamoeba* species; however, no eIF2α kinases have been characterized. In this study, we identified two eIF2α kinases in *E. invadens*, EiIF2K-A and EiIF2K-B. Their identity as eIF2α kinases was validated using a heterologous yeast system. We used an RNA interference (RNAi) trigger-mediated silencing system to reduce expression of EiIF2K-A, which also reduced expression of EiIF2K-B. Parasites with decreased kinase expression exhibited decreased phosphorylation of eIF2α and increased sensitivity to oxidative stress. Diminished kinase expression also correlated with an increased rate of encystation, a decreased rate of excystation, and an increase in several virulence functions, erythrophagocytosis and adhesion to host cells. Taken together, these data suggest that EiIF2K-A and EiIF2K-B are authentic eIF2α kinases that may regulate the *Entamoeba* stress response.

IMPORTANCE *Entamoeba histolytica* is a human pathogen that causes dysentery and affects millions of people worldwide. This parasite possesses a two-stage life cycle: an environmentally stable cyst and the pathogenic trophozoite. Cysts are ingested from contaminated food and water; thus, this parasite in prevalent in underdeveloped countries. Current therapies commonly cause adverse side effects; therefore, new treatments are needed. In the host, *Entamoeba* experiences stress brought on, in part, by the host immune system. Understanding stage conversion and the stress response of this pathogen may lead to new drug therapies. Using the model organism *E. invadens*, we identified two kinases similar to those involved in stress and stage conversion in other systems. We determined that these kinases may regulate the oxidative stress response, stage conversion, and virulence. This work is significant, as it will inform future studies on the life cycle and pathogenicity of *Entamoeba* species.

KEYWORDS *Entamoeba histolytica*, dysentery, eIF2 alpha, encystation, host-parasite adhesion, oxidative stress, phagocytosis, stress adaptation, stress kinases

Editor Ira J. Blader, University at Buffalo

Address correspondence to Lesly A. Temesvari, LTEMESV@clemson.edu.

The authors declare no conflict of interest.

Received 3 March 2022
Accepted 3 May 2022
Published 31 May 2022

Entamoeba histolytica is a human pathogen that causes amoebiasis and amoebic liver abscess, affecting millions of people worldwide and causing an estimated 55,000 deaths annually (1). *E. histolytica* has a two-stage life cycle: the infectious cyst and the pathogenic amoeboid trophozoite. Latent cysts are ingested from fecally contaminated food or water; thus, this parasite is prevalent in underdeveloped countries, where infrastructure, especially sanitation, is substandard. In 2015, 663 million people lacked access to clean drinking water and almost 1 billion people still practiced open defecation (2). Additionally, amoebiasis is the leading cause of diarrheal disease in travelers returning to the United States (1). Considered together, these characteristics demonstrate that *E. histolytica* constitutes a significant global health problem.

After ingestion, cysts traverse the stomach and enter the small intestine, where unknown cues trigger the excystation of trophozoites. These amoebae travel to the colon, where infection can progress along several nonmutually exclusive routes. The trophozoites may establish a noninvasive infection, feeding on gut flora or host cells by phagocytosis. The parasites may also adhere to and degrade the gut epithelial lining, causing a diarrheal disease known as amoebic dysentery. Occasionally, the parasites breach the intestinal wall, enter the bloodstream, and establish extraintestinal infection in the liver (amoebic liver abscess) or, more rarely, in the lungs and brain. In the large intestine, unknown signals trigger the conversion of trophozoites into environmentally stable mature cysts that are shed into the environment to facilitate host-to-host spread (3). While navigating the human host, *E. histolytica* faces numerous stresses, such as nutrient deprivation, oxidative stress, nitrosative stress, and heat shock (4, 5). To survive, the parasite must surmount these damaging conditions.

Entamoeba invadens, a reptilian parasite, has served as a model to study stage conversion in this genus because it readily encysts and excysts in culture (6–8). Stage conversion is thought to be a response to stress encountered in the colon, and many of the features of the stress response overlap with those of stage conversion. For example, both heat shock proteins and cyst wall proteins are upregulated during heat shock in *E. invadens* (9). Additionally, a eukaryotic type IIA topoisomerase is upregulated during oxidative stress, heat shock, and encystation (10). Given the importance of stress management during the parasite's life cycle, stress response pathways may represent a novel targetable vulnerability. Thus, it is crucial to understand the molecular mechanisms that regulate the parasite stress response. Such information would provide significant insight into *Entamoeba* pathogenicity and would inform future studies focused on antiparasitic drug design.

In most organisms, one branch of the stress response is characterized by the phosphorylation of a conserved serine residue in the alpha subunit of eukaryotic initiation factor-2 (eIF2α). eIF2α is a component of a ternary complex with GTP and the initiator methionyl tRNA (Met-tRNAi). This ternary complex binds the 40S ribosomal subunit, delivering Met-tRNAi for translation initiation. Phosphorylation of eIF2α during stress inhibits this activity, causing a sharp decline in global protein synthesis and preferential translation of a subset of mRNAs that encode stress-related regulators. This process of translational control allows cells to conserve resources and reconfigure gene expression to effectively counter stress. In mammalian cells, phosphorylation of eIF2α is regulated by a family of four eIF2α kinases (GCN2, PKR, PERK, and HRI) that are activated in a stress-specific manner. GCN2 is activated by nutrient starvation, PKR is activated in response to viral infections, PERK is activated by misfolded proteins, and HRI is activated by heme starvation (11). Although translational control, via eIF2α phosphorylation, has been shown to exist in *E. histolytica* (4, 5), no eIF2α kinases have been characterized in *Entamoeba* species.

In this study, we identified two putative eIF2α kinases, EiIF2K-A and EiIF2K-B, in *E. invadens*. We used a heterologous yeast system (12, 13) to confirm that EiIF2K-A and EiIF2K-B are *bona fide* eIF2α kinases. We used a trigger-mediated silencing approach (14) to knock down expression of EiIF2K-A, which simultaneously reduced expression of EiIF2K-B. Parasites with reduced expression of these kinases exhibited decreased levels of phosphorylated eIF2α, a diminished ability to surmount oxidative stress, and altered rates of stage conversion. Furthermore, decreased kinase expression was

correlated with an increase of two virulence functions, erythrophagocytosis and adhesion. Taken together, these data show that EiIF2K-A and EiIF2K-B are authentic eIF2α kinases that may be involved in the parasite stress response, stage conversion, and virulence.

RESULTS

The *E. invadens* and *E. histolytica* genomes each encode two putative eIF2α kinases. Using the amino acid sequences of the four human eIF2α kinases, we searched the *E. invadens* genome (https://amoebadb.org) for candidate sequences that contained hallmarks of eIF2α kinases (15). We found two presumptive *E. invadens* eIF2α kinases, which we named EiIF2K-A (EIN_052050, formerly labeled EIN_033330) and EiIF2K-B (EIN_096010, formerly labeled EIN_059080), which share ~33.5% identity and ~48.1% similarity with each other within their kinase domains (see Table S1 in the supplemental material). According to RNA sequencing data, reported as transcript abundance in transcripts per million (TPM) (https://amoebadb.org), these kinases exhibit stage-specific expression. EiIF2K-A is predominantly expressed in trophozoites and at 48 h into encystation, while EiIF2K-B is expressed only during stage conversion, at low levels during encystation, and at higher levels during excystation (8). Like the genome of *E. invadens*, the genome of the human pathogen, *E. histolytica* also possesses two putative eIF2α kinases, which we named EhIF2K-A (EHI_035950) and EhIF2K-B (EHI_109700). We aligned the putative *Entamoeba* kinase domains with those of other known eIF2α kinases, as well as with that of a control kinase, human CDK1, which does not belong to the family of eIF2α kinases, and noted the similarity and identity (Table S1). The kinase domain of EiIF2K-A shares ~49.9% identity (~64.6% similarity) and ~28.1% identity (~43.9% similarity) with the kinase domains of EhIF2K-A and EhIF2K-B, respectively (Table S1). The kinase domain of EiIF2K-B shares ~31.1% identity (~45% similarity) and ~48.4% identity (~64.9% similarity) with the kinase domains of EhIF2K-A and EhIF2K-B, respectively (Table S1). The kinase domains of EiIF2K-A and EiIF2K-B also share at least 16.57% identity and at least 28.57% similarity with the human eIF2α kinases (Table S1).

The *Entamoeba* kinases possess all 11 subdomains characteristic of the eIF2α kinase family, with highly conserved residues making them more closely related to eIF2α kinases than to the control kinase, CDK1. For clarity, only the alignment for subdomain II, which possesses the critical lysine required for catalytic activity, is shown (Fig. S1). The *Entamoeba* kinases share little homology with other members of this kinase family beyond the kinase domains. A phylogenetic analysis of eIF2α kinases showed that both EiIF2K-A and EiIF2K-B were more closely related to each other and to their *E. histolytica* counterparts (EhIF2K-A and EhIF2K-B) than to any of the other kinases. Additionally, the *Entamoeba* kinases were more closely related to PKR- and PERK-related kinases than to GCN2- or HRI-related kinases (Fig. S2).

EiIF2K-A and EiIF2K-B regulate phosphorylation of eIF2α in a heterologous system. To validate that EiIF2K-A and EiIF2K-B are eIF2α kinases, we utilized a yeast model system that uses *Saccharomyces cerevisiae* strain H1894, in which the sole endogenous eIF2α kinase is deleted. Exogenous expression of authentic eIF2α kinases in this yeast strain results in phosphorylation of endogenous eIF2α. (12, 13, 16). A truncated cDNA encoding the catalytic domain of EiIF2K-A or EiIF2K-B was inserted into the yeast expression vector pYES-NT/C, which confers uracil prototrophy and allows for galactose-inducible expression of exogenous genes (13). The pYES-NT/C plasmid also adds a polyhistidine tag to the N-terminus of the expressed protein. A pYES-NT/C vector lacking an insert (empty pYES) was used as a control plasmid, and the pYES2 plasmid harboring the active kinase domain of human PKR was used as a positive control (13). A standard transformation protocol (17) was used to introduce the expression vectors into the H1894 strain, and transformants were selected by growth on medium that lacked uracil.

Expression of exogenous protein was induced by plating yeast cells on galactose-containing medium. Western blot analysis using an anti-polyhistidine antibody demonstrated successful induction of exogenous protein expression with little to no expression prior to

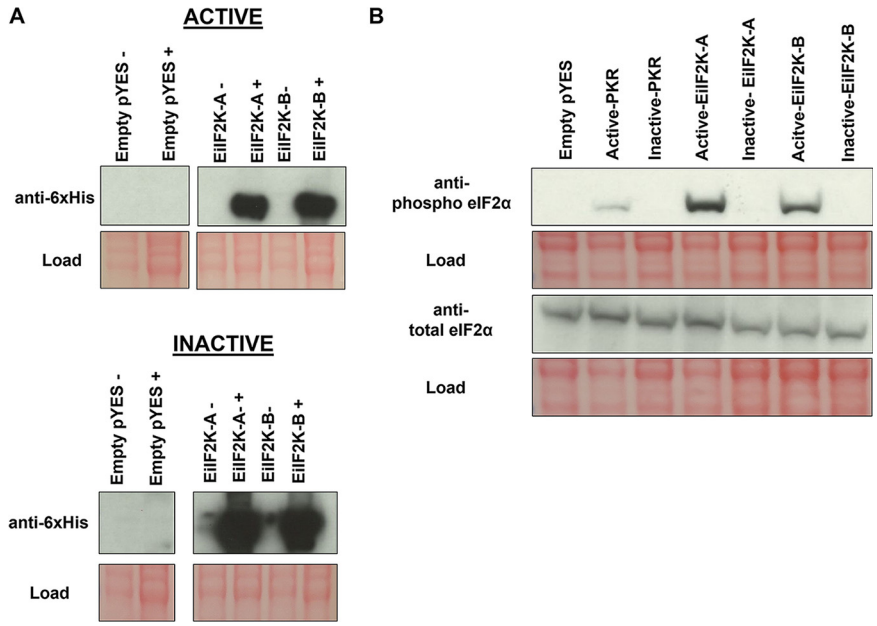

FIG 1 Expression of EiIF2K-A and EiIF2K-B kinase domains in a heterologous yeast system demonstrates kinase activity. Yeast strain H1894, which contains a genetic deletion of its sole eIF2α kinase, was transformed with the galactose-inducible pYES expression vector (empty pYES) or the same vector harboring wild-type (active) or mutated (inactive) coding sequences for EiIF2K-A or EiIF2K-B kinase domains. For the inactive kinases, a conserved lysine in each kinase subdomain II was mutated to arginine to create an inactive kinase. (A) Western blotting, using anti-polyhistidine tag antibody, confirmed galactose-inducible protein expression. −, strains grown on glucose as a carbon source; +, strains grown on galactose as a carbon source. Expression of the EiIF2K-A or EiIF2K-B kinase domains (active or inactive) was evident only when cells were grown on galactose. (B) Western blot showing the level of phosphorylated eIF2α and total eIF2α in H1894 yeast strain harboring empty pYES, a control eIF2α kinase, human PKR (pYES-PKR) (active or inactive) (13), pYES-EiIF2K-A (active or inactive), or pYES-EiIF2K-B (active or inactive). Hyperphosphorylation of eIF2α was observed only in the yeast expressing active kinase domains. Ponceau red staining of membranes (red) indicates load.

exposure to galactose (Fig. 1A). We used Western blotting to assess the level of phosphorylated and total eIF2α in the transgenic yeast strains expressing EiIF2K-A, EiIF2K-B, empty pYES, or human PKR. Both *E. invadens* kinases phosphorylated endogenous yeast eIF2α (Fig. 1B), demonstrating that EiIF2K-A and EiIF2K-B have eIF2α kinase activity.

EiIF2K-A and EiIF2K-B possess the conserved lysine in kinase subdomain II (Fig. S1) that is critical for catalytic activity (18). For a control, we mutated this key lysine residue to arginine in each of the kinases and expressed these "inactive" kinases in the H1894 yeast strain. Western blotting confirmed that inactive kinases were expressed (Fig. 1A) but not capable of phosphorylating yeast eIF2α (Fig. 1B). These findings further support the notion that EiIF2K-A and EiIF2K-B are authentic eIF2α kinases.

EiIF2K-KD parasites exhibit lower phospho-eIF2α levels and altered growth in nutrient-rich medium. We used an RNA interference (RNAi) trigger-mediated gene silencing approach to reduce the expression of EiIF2K-A (14). Since the coding sequence of EiIF2K-A is large (2,727 nucleotides), we subcloned a partial cDNA encoding amino acids 1 to 267, which contains the kinase domain, into the gene silencing trigger plasmid. The trigger plasmid facilitates the production of small interfering RNAs to its insert, which target and bind endogenous mRNA, leading to mRNA degradation via the dicer pathway (14). Complete cDNAs are not required for efficient knockdown using this system (14). Plasmid DNA was transfected into wild-type (WT) *E. invadens* parasites via electroporation, and stable transfectants (EiIF2K-KD) were selected for and maintained by growth in the presence of neomycin. Parasites harboring the trigger plasmid with an insert encoding luciferase, an irrelevant protein, was used as a control (Trig Luc). Using this approach, we obtained substantial knockdown of EiIF2K-A mRNA levels in trophozoites as assessed by reverse transcription (RT)-PCR analysis (Fig. 2A). Additionally, we measured EiIF2K-A expression during stage conversion in control and knockdown parasites. We found that EiIF2K-A mRNA was undetectable in

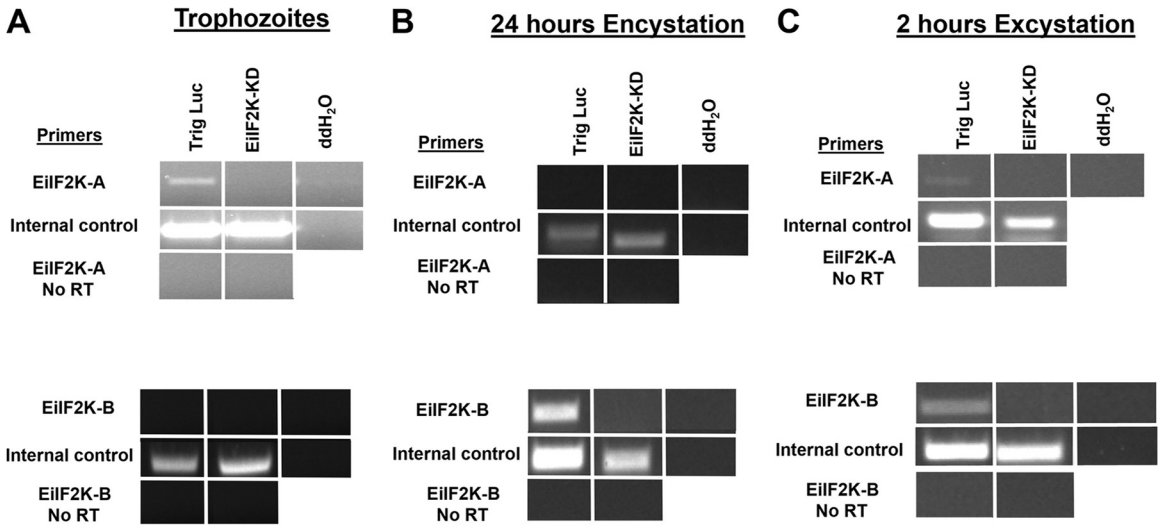

FIG 2 Trigger-mediated knockdown of EiIF2K-A and EiIF2K-B expression during growth and stage conversion. (RT)-PCR was used to measure the level of EiIF2K-A or EiIF2K-B mRNA in transfected parasites harboring the trigger-EiIF2K-A plasmid (EiIF2K-KD) or the trigger-Luc control plasmid (Trig Luc). (A) EiIF2K-A mRNA is undetectable in trophozoites harboring the trigger-EiIF2K-A plasmid. Consistent with the report of Ehrenkaufer et al. (8), expression of EiIF2K-B mRNA is undetectable in the trophozoite stage of *E. invadens*. (B) Consistent with the report of Ehrenkaufer et al. (8), EiIF2K-A mRNA is undetectable in control and mutant parasites at 24 h into encystation. However, a decrease in EiIF2K-B mRNA was observed in the mutant parasites (compared to control) during encystation. (C) Low levels of EiIF2K-A and EiIF2K-B mRNA are detectable at 2 h into excystation in Trig Luc parasites but not in EiIF2K-KD parasites. EIN_192230 or EIN_162500 served as load controls for trophozoites or encysting cells, respectively. No RT reactions eliminated reverse transcriptase to confirm that there was no genomic DNA (gDNA) contamination in cDNA samples. "ddH_2O" indicates reactions in which ddH_2O was used as the template. A lack of product in these reactions confirms no gDNA contamination in the reagents.

control and knockdown parasites during encystation (Fig. 2B). EiIF2K-A mRNA was expressed at low levels in the control Trig Luc parasites at 2 h into excystation but was undetectable in the EiIF2K-KD parasites (Fig. 2C). Since closely related genes may simultaneously be silenced by RNAi approaches (14), it was necessary to also measure expression of EiIF2K-B during growth and stage conversion. EiIF2K-A and EiIF2K-B share 32.64% amino acid identity within the kinase domain (Table S1). Consistent with published transcriptomic data (8), expression of EiIF2K-B was undetectable in control or mutant trophozoites growing in nutrient-rich medium (Fig. 2A). On the other hand, the level of EiIF2K-B mRNA was reduced during both encystation (Fig. 2B) and excystation (Fig. 2C) in the EiIF2K-KD parasites compared to that of the Trig Luc control parasites, suggesting that reducing the expression of EiIF2K-A simultaneously reduced expression of EiIF2K-B during stage conversion.

Previously, we showed that *E. histolytica* parasites possess a basal level of phosphorylated eIF2α, which increases after exposure to a subset of stressful conditions (4, 5) and during encystation (4). Therefore, we measured the level of phosphorylated eIF2α relative to total eIF2α in both trophozoites and encysting control and EiIF2K-KD parasites (Fig. 3). In agreement with previously published data (4), Trig Luc control parasites exhibited a basal level of phosphorylated eIF2α, which increased at 48 and 72 h into encystation (Fig. 3A and B). In contrast, parasites with diminished kinase expression displayed decreased, albeit slightly variable, levels of phosphorylated eIF2α in trophozoites and in encysting parasites. The most dramatic decrease in phosphorylation of eIF2α was observed in the mutant at 48 h into the stage conversion program. While mRNA levels of EiIF2K-A and EiIF2K-B are undetectable by (RT)-PCR in our knockdown cell line (Fig. 1), there must be some remaining level of kinase mRNA expression, as we see some phosphorylation of eIF2α in EiIF2K-KD parasites (Fig. 3A and B). Overall, these data demonstrate that EiIF2K-KD parasites have a reduced capacity for phosphorylating eIF2α, supporting the identity of EiIF2K-A and EiIF2K-B as eIF2α kinases.

We also measured the growth rate of Trig Luc and EiIF2K-KD parasites in both standard nutrient-rich medium and nutrient-poor/low-osmolarity encystation medium for up to 72 h postinoculation (Fig. 3). EiIF2K-KD parasites exhibited a lag in growth when seeded into

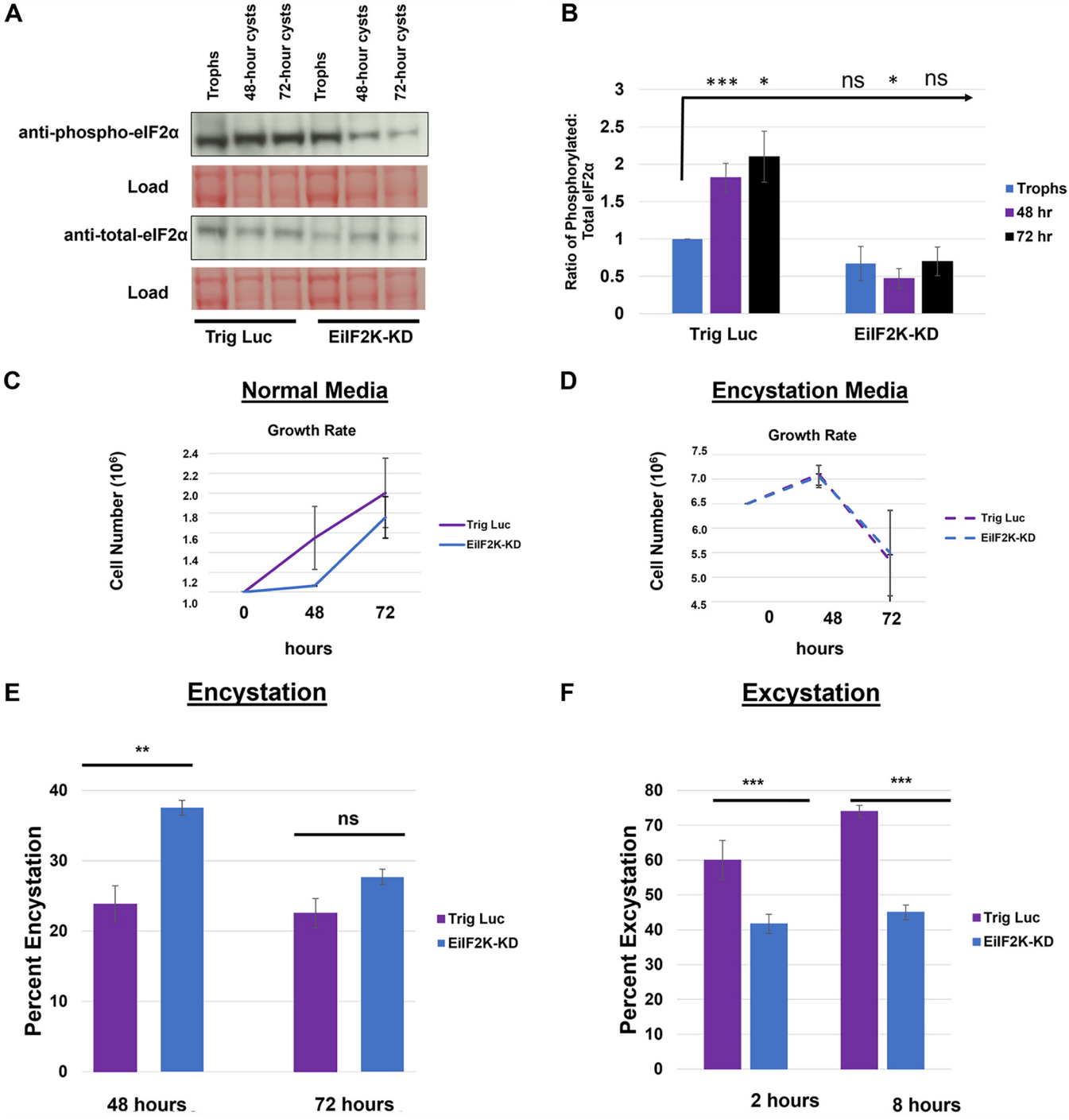

FIG 3 EilF2K-KD parasites exhibit reduced phosphorylation of eIF2α, reduced growth in nutrient-rich medium, and altered rates of stage conversion. The level of phosphorylated and total eIF2α in Trig Luc and EilF2K-KD parasites was measured during growth and encystation by Western blotting using antibodies specific for phosphorylated or total eIF2α. Levels of protein were quantified using scanning densitometry of bands on the same blot (ImageJ), and the ratio of phosphorylated eIF2α to total eIF2α was calculated after correcting for load. (A) Representative Western blots for control (Trig Luc) or knockdown (EilF2K-KD) trophozoites (Trophs) and encysting parasites. (B) Ratio of phosphorylated eIF2α to total eIF2α for Trig Luc or EilF2K-KD trophozoites (blue), 48-h cysts (purple), and 72-h cysts (black). The ratio for Trig Luc trophozoites was arbitrarily set to 1.0 and was used as the basis for comparison. During encystation, the ratio of phosphorylated eIF2α to total eIF2α increases in Trig Luc parasites ($P < 0.05$). In all stages of the life cycle, the ratio of phosphorylated eIF2α to total eIF2α was generally decreased in EilF2K-KD parasites compared to that in Trig Luc parasites. The most dramatic decrease in the ratio of phosphorylated to total eIF2α was observed in the mutant at 48 h into the encystation program ($P < 0.05$). ns, not statistically significant. Data represent the mean $\pm$ standard error of at least 5 separate trials. (C and D) Trophozoites were seeded into 13 mL standard nutrient-rich culture medium (1×10^6 initial inoculum) (C) or into 13 mL encystation medium (6.5×10^6 initial inoculum) (D) in 15-mL screw-cap tubes and incubated at 25°C for 48 or 72 h. At each time point, parasites were enumerated using trypan blue (1 mg/mL) exclusion and light microscopy. (C) EilF2K-KD parasites exhibit an initial lag in growth when seeded into nutrient-rich medium but eventually show an increased growth rate between 48 and 72 h compared to

(Continued on next page)

nutrient-rich medium but eventually exhibited a higher rate of growth than control parasites (Fig. 3C). This growth phenotype, exhibited by EiIF2K-KD parasites in nutrient-rich medium, was likely the result of reduced EiIF2K-A expression, as it is the only kinase expressed in trophozoites. On the other hand, there was no difference in the growth kinetics of the mutant in encystation medium compared to that of the control parasites (Fig. 3D). The decrease in parasite number during incubation in encystation medium (Fig. 3C and D) is typical, as a fraction of the population loses viability instead of encysting.

EiIF2K-KD parasites have altered rates of stage conversion. To elucidate the role of the kinases in stage conversion, we measured the rate of encystation and excystation in both Trig Luc and EiIF2K-KD parasites. Encystation was induced by inoculating parasites into nutrient-poor/low-osmolarity encystation medium. Hallmarks of encystation include the accumulation of a chitin-rich cell wall and a reduction in cell size (19). To assess encystation, we used flow cytometry (19) and Congo red staining to track the accrual of chitin as well as changes in cell size. In the EiIF2K-KD parasites, the percentage of parasites that had encysted was significantly higher than that of control parasites at 48 h postinoculation, but not at 72 h postinoculation (Fig. 3E). This suggests that the rate, but not the overall efficiency, of encystation is higher in parasites with diminished kinase expression. Since both kinases are expressed during encystation, we cannot discern if the encystation phenotype is due to loss of one or both kinases. To induce excystation, cysts were incubated in excystation medium, which restores nutrients and osmolarity and contains bile salts to mimic passage through the host digestive system (8). EiIF2K-KD parasites exhibited a significantly lower rate of excystation than control parasites at 2 h and 8 h into the excystation program (Fig. 3F). Since EiIF2K-B is the only kinase expressed during excystation, we posit that reduced EiIF2K-B expression is responsible for this excystation phenotype.

EiIF2K-KD trophozoites are more susceptible to oxidative stress. Previously, we demonstrated that *E. histolytica* phosphorylates eIF2α in response to several different stressful conditions, including oxidative stress (4). As such, EiIF2K-A, the sole kinase expressed in trophozoites, may be responsible for countering oxidative stress. Suresh et al. demonstrated that exposing *E. invadens* parasites to 4 mM H_2O_2 for 1 h induced oxidative stress, as evidenced by detachment and rounding of parasites, while maintaining $\geq$90% viability (14). However, the level of phospho-eIF2α in H_2O_2-treated *E. invadens* trophozoites has not been examined. Therefore, we exposed WT *E. invadens* trophozoites to double distilled water (ddH_2O) (diluent) or 4 mM H_2O_2 for 1 h at 25°C and measured the levels of total and phosphorylated eIF2α by Western blotting (Fig. S3A). Phosphorylation increased in parasites treated with 4 mM H_2O_2 compared to that in the unstressed control. To ascertain if EiIF2K-A regulates the response to oxidative stress in trophozoites, we measured the viability of WT, Trig Luc, and EiIF2K-KD parasites exposed to 4 mM H_2O_2; however, we observed no difference in viability (Fig. S3B). Therefore, we used a higher concentration of H_2O_2 that could reduce viability of WT *E. invadens* parasites. WT, Trig Luc, and EiIF2K-KD parasites were exposed to 1 M H_2O_2 for 1 h at 37°C. This treatment caused approximately 30% parasite death in WT parasites, 40% parasite death in Trig Luc parasites (Fig. 4A), and approximately 65% parasite death in EiIF2K-KD parasites. The statistically significant reduction in viability in EiIF2K-KD parasites supports the notion that EiIF2K-A may regulate the response to oxidative stress in *E. invadens* trophozoites.

EiIF2K-KD parasites may be more susceptible to oxidative stress because of their reduced capacity to phosphorylate eIF2α. Thus, we used Western blotting to measure the levels of phosphorylated and total eIF2α in control and EiIF2K-KD parasites

FIG 3 Legend (Continued)
that of Trig Luc parasites. (D) EiIF2K-KD and Trig Luc parasites show no difference in growth rate at 48 or 72 h. Data represent the mean $\pm$ standard error of at least 3 separate trials. (E) Trig Luc and EiIF2K-KD parasites were induced to encyst for either 48 or 72 h. Mature cysts were stained with Congo red and quantified using flow cytometry. A higher percentage of EiIF2K-KD parasites than of Trig Luc parasites encysted by 48 h and by 72 h. However, the increase was statistically significant only at 48 h ($P < 0.01$), suggesting that the mutants have a higher initial rate of encystation but not a higher efficiency of encystation. (F) Trig Luc cells and EiIF2K-KD cysts were induced to excyst by incubation in excystation medium for 2 or 8 h. The number of mature cysts was quantified before and after excystation, and the decrease in the number of cysts represents the fraction (percent) of parasites that had excysted. The excystation rate of EiIF2K-KD was significantly ($P < 0.001$) lower than that of Trig Luc parasites at both 2 and 8 h. Data represent the mean $\pm$ standard error of at least 3 separate trials.

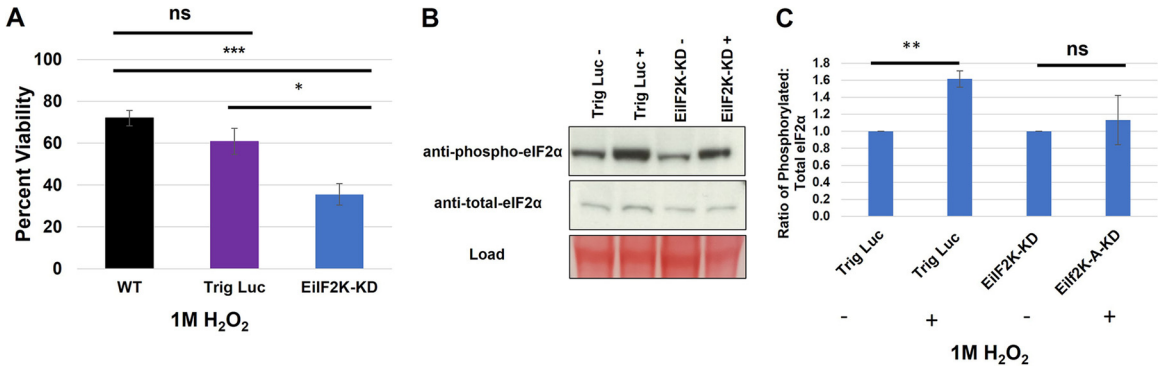

FIG 4 EiIF2K-KD trophozoites are more susceptible to oxidative stress. Wild-type (WT), Trig Luc, or EiIF2K-KD trophozoites were exposed to 1 M H_2O_2 for 1 h at 25°C. (A) Viability was assessed using trypan blue exclusion and a Luna automated cell counter. EiIF2K-KD parasites were significantly less viable when exposed to oxidative stress than WT ($P < 0.001$) and Trig Luc parasites ($P < 0.05$). (B) Representative Western blot showing the level of phosphorylated and total eIF2α in Trig Luc or EiIF2-KD cells before (−) and after (+) H_2O_2 treatment. (C) Western blotting was used to measure the levels of total and phosphorylated eIF2α in parasites exposed to ddH_2O or 1 M H_2O_2 for 1 h at 25°C. Levels of protein were quantified using scanning densitometry of bands on the same blot (ImageJ), and the ratio of phosphorylated eIF2α to total eIF2α was calculated after correction for load. Trig Luc parasites exposed to 1 M H_2O_2 exhibited significantly higher ($P < 0.01$) levels of phosphorylated eIF2α than controls, while EiIF2K-KD parasites exposed to the same conditions did not exhibit significantly increased levels of phosphorylated eIF2α. Data represent the mean ± standard error of at least 3 separate trials.

exposed to H_2O_2. The ratio of phosphorylated eIF2α to total eIF2α increased significantly in stressed Trig Luc parasites but not in EiIF2K-KD parasites (Fig. 4B and C). There is a slight increase in phosphorylation of eIF2α in EiIF2K-KD parasites treated with 1M H_2O_2 compared to those parasites treated with ddH_2O. Currently, there are no methods to knock out genes in *Entamoeba* species. Therefore, there remains some level of kinase expression in our EiIF2K-KD parasites, which may respond to stress. Overall, these data support the identity of EiIF2K-A as an authentic kinase and emphasize the importance of the eIF2α mechanism in parasite stress management.

EiIF2K-KD trophozoites exhibit increased virulence functions. To discern the effect of decreased EiIF2K-A expression on parasite virulence, we measured two key virulence functions: erythrophagocytosis and adhesion to host cells. Trig Luc and EiIF2K-KD trophozoites were exposed to human red blood cells (hRBCs) for 10 min, after which uptake of heme was quantified spectrophotometrically (20). Adhesion was measured by quantifying the degree to which fluorescently labeled parasites adhered to a fixed monolayer of Chinese hamster ovary (CHO) cells (21). EiIF2K-KD parasites exhibited significantly increased phagocytosis (Fig. 5A) and adhesion (Fig. 5B), which suggests that EiIF2K-A may directly or indirectly modulate virulence functions, as EiIF2K-A is the only eIF2α kinase expressed by trophozoites.

DISCUSSION

This is the first study to characterize eIF2α kinases in *Entamoeba* species. We used a heterologous yeast system to show that EiIF2K-A and EiIF2K-B are authentic eIF2α kinases. Using an established RNAi silencing approach (14), we knocked down both kinases using a single trigger-EiIF2K-A plasmid. We found that EiIF2K-KD parasites were more susceptible to oxidative stress and exhibited increased virulence functions (erythrophagocytosis and parasite-host cell adhesion). We also observed an increased rate of encystation and a decreased rate of excystation in EiIF2K-KD parasites. Due to the stage-specific expression patterns of these kinases, we posit that EiIF2K-A may regulate phenotypes observed in trophozoites, while the excystation phenotype may be due to the loss of EiIF2K-B. Overall, this study advances our knowledge about the stress response and stage conversion in *Entamoeba* species.

In mammalian cells, phosphorylation of eIF2α is regulated by a family of four eIF2α kinases that are activated in a stress-specific manner. The ability of the kinases to respond to various stresses relies on regulatory domains. Interestingly, in several protozoan parasites (13, 22–24), the eIF2α kinases possess divergent regulatory domains, suggesting that protozoan eIF2α kinases may respond differently to environmental stress than their

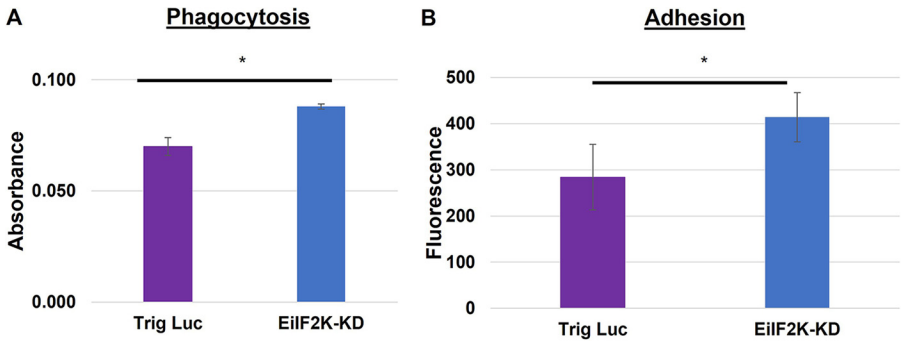

FIG 5 Erythrophagocytosis and adhesion are increased in EiIF2K-KD parasites. (A) Trig Luc or EiIF2K-KD parasites were incubated with human red blood cells (hRBC-to-amoeba ratio, 100:1) for 10 min, lysed, and spectrophotometrically analyzed for internalized heme at 405 nm. Amoebae with reduced expression of EiIF2K-A exhibited increased phagocytosis of hRBCs. The data represent the mean ± standard error of at least 3 separate trials ($P < 0.05$). (B) Calcein AM-stained control or mutant parasites were incubated with fixed monolayers of Chinese hamster ovary (CHO) cells for 30 min. Unadhered parasites were rinsed off the monolayer of CHO cells, and the level of adhesion (calcein-AM fluorescence) was measured by spectrofluorimetry using an excitation wavelength of 485 nm and an emission wavelength of 528 nm. EiIF2K-KD trophozoites exhibited significantly higher adhesion to host cells than Trig Luc trophozoites ($P < 0.05$). Data represent the mean ± standard error of at least 3 separate trials.

mammalian counterparts (11). Currently, it is not possible to predict, by sequence analysis, the types of stresses to which the *Entamoeba* kinases will respond.

Nevertheless, we demonstrate that trophozoites with reduced EiIF2K-A expression are more susceptible to at least one stressful condition, oxidative stress. EiIF2K-KD parasites were less viable in the presence of high concentrations of H_2O_2 and possessed decreased levels of phosphorylated eIF2α compared to control parasites (Fig. 4A). This is not surprising, since Hendrick et al. (4) demonstrated that oxidative stress induces the phosphorylation of eIF2α in *E. histolytica*. Likewise, Augusto et al. (25) knocked out an eIF2α kinase in *Toxoplasma gondii*, TgIF2K-B, and found that null parasites had an impaired response to oxidative stress. To further illuminate the stress-specific response of this kinase, it will be necessary to assess the ability of the EiIF2K-KD cells to survive other stressful conditions. Additionally, examining the transcriptome and translatome of EiIF2K-KD and control parasites under oxidative stress would help to determine if these eIF2α kinases directly regulate the stress response of *E. histolytica*.

EiIF2K-KD parasites exhibited no growth phenotype in encystation medium and a transient lag in growth in nutrient-rich medium (Fig. 3C and D). This is unlike *Trypanosoma cruzi* parasites lacking the eIF2α kinase, TcK2, which exhibit a growth deficiency (26). However, the *E. invadens* phenotype is similar that of *Leishmania donovani* parasites expressing a dominant negative version of a GCN2-like kinase, which do not exhibit a growth defect (22). It is possible that in *L. donovani*, multiple eIF2α kinases share redundant functions and that the loss of one kinase is compensated for by other related kinases. However, in *E. invadens*, EiIF2K-A is the only eIF2α kinase expressed in trophozoites (see reference 8 and the present study). Thus, compensation by related kinases may not be possible in the trophozoite stage of this parasite.

EiIF2K-A is expressed in trophozoites and decreases during initial encystation (8). Since decreased EiIF2K-A expression correlates with initiation of encystation, it is conceivable that EiIF2K-KD parasites are primed to encyst. In support of this, the encystation rate of the EiIF2K-KD parasites was significantly higher than that of control parasites at 48 h (Fig. 3E). If EiIF2K-KD parasites are primed to encyst, they may exhibit early expression of encystation-specific genes, which, in turn, could lead to an increased rate of encystation, but not necessarily an increased efficiency. To gain further insight into the relationship between eIF2α kinase expression and encystation, it will be necessary to define the cyst-specific translatome, perhaps by ribosome profiling (Ribo-seq) (27), in EiIF2K-KD trophozoites.

The excystation rate of EiIF2K-KD parasites was significantly decreased (Fig. 3F). EiIF2K-B is expressed at low levels during encystation and at high levels during excystation (8).

Therefore, we hypothesize that the excystation phenotype may be due to the loss of EiIF2K-B, as it is the only eIF2α kinase expressed during excystation. At present, we cannot determine if the encystation phenotype is due to loss of EiIF2K-A, EiIF2K-B, or both. Nevertheless, stage conversion was not completely disabled. One possibility is that residual levels of EiIF2K-A and/or EiIF2K-B are sufficient to maintain stage conversion, albeit at rates that differ from wild-type rates. Although our bioinformatics search of kinases was robust, we also cannot rule out the possibility that there is an additional eIF2α kinase. A third possibility is that there may be an unknown compensatory mechanism operating to affect stage conversion. Comparing the transcriptomes of these cell lines would help illuminate this pathway. To understand the exact roles of EiIF2K-A and EiIF2K-B in stage conversion, it will be essential to knock down each gene individually and evaluate stage conversion.

Previously, we demonstrated that the level of phosphorylated eIF2α increases significantly during encystation (4). Thus, it was not surprising that EiIF2K-A and/or EiIF2K-B may play a role in stage conversion in *E. invadens*. Likewise, eIF2α kinases play roles in stage conversion in other protozoa. For instance, phosphorylation of eIF2α increases during stage conversion or differentiation of *Trypanosoma cruzi* (26, 28), *T. gondii* (29), and *Plasmodium falciparum* (23). It was unanticipated that reduced phosphorylation of eIF2α would correlate with an increased rate of encystation in *E. invadens*. Perhaps in *Entamoeba* species, precise timing of translation is necessary to control the rate of encystation in such a way as to guarantee the accurate conversion of trophozoites into environmentally stable cysts. Without the kinases that control phosphorylation of eIF2α, the rate of translation becomes unbridled, and the rate of encystation becomes unregulated.

EiIF2K-KD parasites exhibited increased erythrophagocytosis and adhesion to host cells, which are two important virulence functions (Fig. 5). These data suggest that EiIF2K-A, the only eIF2α kinase expressed in trophozoites (8), may directly or indirectly regulate erythrophagocytosis and adhesion. Similarly, *T. gondii* parasites lacking one eIF2α kinase, TgIF2K-B, were more virulent *in vivo* (25). Given the role of eIF2α kinases in the management of translation, one explanation for increased parasite virulence functions is dysregulated translation of genes that control virulence.

It may be argued that an increase in virulence functions or the rate of encystation in the EiIF2K-KD parasites implies that this kinase is not a suitable target for antiparasitic drug design. However, increased sensitivity to oxidative stress in the EiIF2K-KD parasites supports its potential as a drug target. *Entamoeba* species are microaerophilic. Therefore, to survive in the host, these parasites must preserve intracellular hypoxia within oxygenated host tissues, such as the liver, and surmount attacks on cellular homeostasis by reactive oxygen species originating from the host immune response (30). Thus, it is conceivable that disabling EiIF2K-A would simultaneously restrict the ability of the pathogen to endure in the host. In support of this, genetic loss of the eIF2α kinases, PERK and GCN2, in immortalized mouse fibroblasts and human tumor cells increases their susceptibility to oxidative stress (31).

The eIF2α kinases are also implicated in human pathologies, including cancer (32), diabetes (33), and neurodegenerative disorders (34), and are the subject of intense study because they represent logical targets for the design of therapies. It has been found that the compound, LDN-0060609, significantly inhibits PERK-mediated phosphorylation of eIF2α in rat astrocytes, which suggests that it may be a suitable drug for the treatment of neurological diseases (35). Targeting the eIF2α-based regulation of translation in protozoan parasites is also under way. For example, pharmacological inhibition of PK4 in *P. falciparum* with the PERK inhibitor, GSK2606414, blocks parasite differentiation and reduces artemisinin-induced latency (36). Inhibition of the PERK-like eIF2 kinase, TgIF2K-A, in *T. gondii*, with the same inhibitor, blocked multiple steps of the tachyzoite lytic cycle and lowered the rate of bradyzoite differentiation (37). Finally, GSK2606414 reduced *Leishmania amazonensis* infection of macrophages (38). Together with the data presented in this study, these encouraging results in other pathogens support the potential for the *Entamoeba* eIF2α kinases to serve as targets for drug inhibition.

MATERIALS AND METHODS

Protein alignment and phylogenetic analysis. The kinase domain sequences of the four putative *Entamoeba* kinases were obtained from UniProt (39). Sequences were also analyzed using ScanProsite (40) to identify the kinase domains and to search for other possible domains and motifs. The catalytic domains of the four putative kinases were aligned with the kinase domains of previously characterized eIF2a kinases using the Clustal W algorithm with standard parameters in SnapGene (version 5.2.1; GSL Biotech, LLC, San Diego, CA, USA). The software Jalview (41) was used to remove the inserts with high length variability for clearer visualization. A phylogenetic analysis was performed using the unedited alignment and the website Méthodes et Algorithmes pour la Bio-informatique LIRMM (http://www.phylogeny.fr/index.cgi) (42). The Newick format of the phylogeny was imported into the Interactive Tree of Life (iTOL) (https://itol.embl.de) (43) to generate the visual tree. All webpages and applications were used with the standard settings for each step. The tree was rooted to the more distantly related sequence of the pool (CDK1).

Strains and culture conditions. *Entamoeba invadens* (strain IP-1) was cultured axenically in TYI-S-33 medium in 15-mL glass screw-cap tubes or 25-cm^2 culture flasks at 25°C (44). Parasites were passaged into fresh medium every 7 days. Chinese hamster ovary (CHO) cells were cultured in Dulbecco's Modified Eagle Medium (DMEM) supplemented with 10% (vol/vol) fetal bovine serum, PenStrep (90 U/mL penicillin, 0.09 μg/mL streptomycin), and HEPES (0.9 mM) in 25-cm^2 treated tissue culture flasks at 37°C and passaged into new flasks every 5 days.

To generate a plasmid to reduce expression of EiIF2K-A, PCR was employed to amplify the kinase domain of EiIF2K-A using genomic DNA as a template and gene-specific primers (see Table S2 in the supplemental material). The primers also added AvrII restriction sites to the 3′ and 5′ ends, which facilitated subcloning into the trigger plasmid (14) (kind gift of Upinder Singh, Stanford University). Successful subcloning was confirmed by sequencing.

E. invadens was transfected by electroporation as described previously (44), with minor modifications. Briefly, two 25-cm^2 flasks containing log-phase trophozoites were iced for 15 min to release adherent parasites. The parasites were collected by centrifugation at 500 $\times$ *g* for 5 min and washed with 20 mL ZM phosphate-buffered saline (PBS) buffer (132 mM NaCl, 8 mM KCl, 8 mM $NaPO_4$, 1.5 mM KH_2PO_4). Parasites were pelleted by centrifugation at 500 $\times$ *g* for 5 min and resuspended in 1.6 mL complete ZM PBS buffer (ZM PBS with 0.5 mM $Mg(CH_3COO)_2 \cdot 4H_2O$ and 0.09 mM $CaCl_2$). Eight hundred microliters of parasite suspension was combined with 150 μg plasmid DNA and electroporated in a 0.4-cm cuvette with two pulses at 1.2 kV and 25 μF using a Bio-Rad Gene Pulser II. Parasites were transferred to 15-mL culture tubes containing 13 mL TYI-S-33 and allowed to recover for 48 h. Neomycin selection was increased gradually at 5 μg/mL each week until a concentration of 50 μg/mL was reached.

To assess expression of EiIF2K-A and EiIF2K-B, RNA was extracted from trophozoites or cysts using TRIzol (Thermo Fisher, Waltham, MA). Two micrograms of total RNA was treated with RQ1 DNase enzyme (Promega, Madison, WI) per the manufacturer's instructions. Treated RNA was used to synthesize cDNA using the Invitrogen Superscript III first stand synthesis kit per the manufacturer's instruction (Thermo Fisher). One microliter of cDNA was used as the template, and PCR was carried out using EiIF2K-A-specific primers or EiIF2K-B gene-specific primers (Table S2). In all cases, 35 cycles were used to amplify PCR products, which were resolved and visualized by electrophoresis on 1% (wt/vol) agarose gels. We also confirmed that these primers do not cross-react to amplify both genes. EIN_327460 was used as an internal load control for analysis of gene expression in trophozoites, and EIN_162500 was used as an internal load control for analysis of gene expression in cysts (Table S2).

Analysis of eIF2 kinase function in yeast. The coding sequences of the kinase domain of EiIF2K-A (1,313 bp) and EiIF2K-B (1,397 bp) were synthesized and ligated into the pYES-NT/C plasmid (Thermo Fisher; kind gift of William Marcotte, Clemson University), by GenScript (Piscataway, NJ, USA), using the restriction enzyme sites BamHI and NotI. The resulting construct contained the kinase domains in-frame with an N-terminal polyhistidine tag, which was confirmed by sequencing. To generate an inactive kinase, the conserved lysine in kinase subdomain II (EiIF2K-A, position 43, and EiIF2K-B, position 45) was mutated to arginine using the Phusion site-directed mutagenesis kit (Thermo-Fisher) and mutagenic primers (Table S2). Successful mutagenesis was confirmed by sequencing. Active and inactive human PKR kinase domains in the yeast expression plasmid, pYES2 (controls), were kind gifts from Ronald Wek (Indiana University School of Medicine).

The pYES-NT/C or pYES2 plasmids encoding the active or inactive kinase domain, or no gene product (empty pYES-NT/C), were introduced into *Saccharomyces cerevisiae* strain H1894 (*MATa ura3-52 leu2-3 leu2-112 gnc2*Δ *trp1*Δ*-63*), which lacks the sole yeast eIF2α kinase, GNC2 (12, 16). Yeast was cultured at 30°C on Yeast Extract-Peptone-Adenine-Dextrose (YAPD) agar plates containing 2% (wt/vol) glucose prior to transformation. Yeast transformation was carried out as described previously (17). Briefly, yeast strain H1894 was inoculated into 5 mL of liquid YPAD medium and grown overnight at 30°C on a rotary shaker at 200 rpm. A total of 250 $\times$ 10^6 cells were inoculated into 50 mL prewarmed 2$\times$ YPAD (2% [wt/vol] Bacto yeast extract, 4% [wt/vol] Bacto peptone, 4% [wt/vol] glucose, 80 mg/L adenine hemisulfate) and incubated at 30°C while shaking at 200 rpm for 4 h. Cells were harvested by centrifugation at 3,000 $\times$ *g* for 5 min and washed twice with sterile water. Cells were harvested by centrifugation at 3,000 $\times$ *g* for 5 min and resuspended in 1 mL sterile water. One hundred microliters of cell suspension was mixed with 360 μL of transformation mix (240 μL polyethylene glycol [PEG] 3350 [50%, wt/vol], 36 μL 1.0 M lithium acetate, 50 μL denatured salmon sperm DNA [2.0 mg/mL], and plasmid DNA [1 μg dissolved in 36 μL sterile water]) in a 1.5-mL microcentrifuge tube and incubated in a 42°C water bath for 40 min. Cells were harvested by centrifugation at 13,000 $\times$ *g* for 30 s and resuspended in 1 mL sterile water. Since pYES-NT/C confers uracil prototrophy to transformants, selection was carried out by plating

transformed yeast cells on agar plates containing synthetic dropout (SD) medium (Sigma-Aldrich, St. Louis, MO, USA) (without uracil) and 2% (wt/vol) glucose and growing them overnight at 30°C.

To induce expression of exogenous protein, cells from each transformed yeast strain were inoculated into liquid SD medium containing 2% (wt/vol) raffinose and 10% (wt/vol) galactose (13) and grown overnight at 30°C prior to Western blotting.

Western blotting. Western blotting of whole-cell lysates was used to assess the expression of kinases in yeast or the level of total and phosphorylated eIF2α in yeast or in *E. invadens*. For yeast, cell lysates were prepared as described previously (45). Briefly, 1.89×10^7 yeast cells were pelleted by centrifugation at 3,000 $\times$ *g* for 5 min. To prepare yeast for lysis, cells were resuspended in 0.5 mL 2 M lithium acetate (Sigma-Aldrich) and incubated on ice for 5 min. Cells were pelleted by centrifugation at 500 $\times$ *g* for 5 min, resuspended in 0.5 mL 0.4 M NaOH, and incubated on ice 5 min. For *E. invadens*, trophozoites or encysting parasites (3×10^5) were pelleted by centrifugation at 500 $\times$ *g* for 5 min. Both yeast cells and *E. invadens* parasites were resuspended in NuPAGE LDS sample buffer (Life Technologies, Carlsbad, CA, USA). An additional step was required to lyse *E. invadens* cysts. Cysts (in NuPAGE LDS buffer) were also exposed to three cycles of freeze-thaw in liquid nitrogen.

For each Western blot, samples were heated for 5 min at 100°C and loaded onto a unique precast NuPAGE 12% Bis-Tris gel (Life Technologies; Carlsbad, CA). The gels were electrophoresed at 180 V for 60 min, and proteins were transferred to polyvinylidene difluoride (PVDF) membranes (Life Technologies) at 12 V for 1.5 h in Towbin transfer buffer (25 mM Tris, 192 mM glycine, 20% [vol/vol] methanol). Prior to blocking, membranes were stained with Ponceau S reagent (Sigma-Aldrich) to record protein load.

The membranes were blocked with 5% (wt/vol) blotting-grade powdered milk blocker (Bio-Rad Laboratories, Hercules, CA) and 0.5% (wt/vol) bovine gelatin (Sigma-Aldrich) in TBST (50 mM Tris, 150 mM NaCl, 0.5% [vol/vol] Tween 20) for 35 min at 37°C. Membranes were incubated overnight at 4°C in primary antibodies (diluted 1:1,000 in TBST). For yeast, the primary antibodies were horseradish peroxidase-conjugated anti-polyhistidine tag antibody (Sigma-Aldrich, St. Louis, MO; kind gift of Michael Sehorn, Clemson University), yeast-specific anti-phosphorylated eIF2α antibody (Thermo Fisher), or yeast-specific anti-total eIF2α antibody (gift of Thomas Dever, NIH). For *E. invadens*, the primary antibodies were *Entamoeba*-specific anti-phosphorylated eIF2α antibody (4) or anti-total eIF2α antibody (4). The membranes were washed in TBST for 45 min with 6 buffer changes. Membranes were incubated in commercially available horseradish peroxidase-conjugated goat anti-rabbit antibody (Thermo Fisher; diluted 1:5,000 in TBST) for 1 h at room temperature and extensively washed as described above. All blots were developed using a commercially available enhanced chemiluminescence Western blotting detection system (Thermo Scientific) according to the manufacturer's instructions. Bands on the same membrane were quantified using scanning densitometry and ImageJ software (version 1.51; NIH).

Induction of stage conversion. To induce encystation, control and mutant trophozoites (6.5×10^6) were pelleted by centrifugation at 500 $\times$ *g* for 5 min and resuspended in 47% (wt/vol) low-glucose/serum-free/high-osmolarity encystation medium (4, 7), supplemented with 50 mg/mL neomycin. Parasites were incubated at 25°C for either 48 h or 72 h, and encystation was tracked by staining with Congo red (Amresco, Solon, OH) and flow cytometry (19). Briefly, encysting *E. invadens* cells were collected over time, stained with the fluorescent chitin stain, Congo red, fixed, and analyzed by flow cytometry using a BD Accuri C6 flow cytometer (BD Biosciences, San Jose, CA) and by collecting 10,000 individual events. To evaluate information about cell size/shape and chitin simultaneously, all data were analyzed using forward scatter (FSC) data versus fluorescence density plots.

Excystation was induced as described previously (8). Briefly, Trig Luc and EiIF2K-KD trophozoites were induced to encyst for 72 h. Parasites were then incubated in 13 mL ddH_2O at 4°C overnight to lyse unencysted trophozoites. Cysts were enumerated using a Luna automated cell counter (Logos Biosystems, Annandale, VA), pelleted by centrifugation at 500 $\times$ *g* for 5 min, resuspended in 13 mL TYI-S-33 medium, 1 mg/mL bile salts (Sigma-Aldrich), and 40 mM $NaHCO_3$, and incubated at 25°C for 2 h or 8 h. After incubation, cultures were iced for 8 min to detach any trophozoites from the glass culture tubes, pelleted by centrifugation at 500 $\times$ *g* for 5 min, resuspended in 1 mL of 1% (vol/vol) Sarkosyl in PBS, and incubated on ice for 30 min to lyse any trophozoites or immature cysts. The remaining detergent-resistant cysts were enumerated, and the percent excystation was calculated by comparing the total cysts remaining to the starting number of cells.

Phagocytosis assays. Phagocytosis assays were carried as previously described (20) with minor changes. Briefly, control or mutant trophozoites were rinsed once in PBS (GE Life Sciences) and twice in serum-free TYI-S-33 medium (SFM). Trophozoites (2×10^5) were resuspended in 150 μL SFM. Freshly isolated human red blood cells (hRBCs) were pelleted by centrifugation (2000 $\times$ *g* for 1 min), rinsed once with PBS and twice with SFM, and resuspended at a concentration of 4×10^5 cells/μL in SFM. hRBCs (2×10^7) were added to the trophozoites and incubated at 25°C for 10 min. Samples were pelleted by centrifugation (2,000 $\times$ *g* for 1 min), and undigested hRBCs were hypotonically lysed by washing twice with 1 mL of ice-cold ddH_2O. Parasites were washed with 1 mL ice-cold PBS, collected by centrifugation (2,000 $\times$ *g* for 1 min), and lysed with 200 μL concentrated formic acid (Fisher). Phagocytosis was measured as the absorbance of heme in the lysate at 405 nm. Sample values were corrected using a formic acid blank.

Adhesion assays. Adhesion assays were carried out as previously described (21) with minor changes. Briefly, control and mutant parasites were incubated with calcein-AM (Invitrogen) (5 μL/mL) for 30 min at 25°C. Chinese hamster ovary (CHO) cells (1.5×10^5) were seeded into a 96-well plate and grown at 37°C for 24 h. CHO monolayers were fixed by incubation with 4% (vol/vol) paraformaldehyde in PBS for 10 min at 37°C. To inactivate paraformaldehyde, the CHO monolayer was incubated with 200 μL of 250 mM glycine for 15 min. Glycine was removed by rinsing with PBS. Calcein-AM-labeled parasites were washed once with SFM at room temperature, and 5×10^4 parasites were seeded onto the

fixed monolayer of CHO cells. Parasites were incubated with fixed CHO cells in SFM for 30 min at 25°C. The medium was carefully aspirated, and the cell layer was gently rinsed twice with PBS at room temperature. The number of adherent parasites was determined by measuring fluorescence at excitation and emission wavelengths of 495 and 525 nm, respectively, with a fluorimeter/plate reader (model FLX800; BioTek Instruments, Winooski, VT).

Induction of oxidative stress. Control or mutant parasites were incubated with 4 mM or 1 M H_2O_2 for 1 h at 25°C. Viability was assessed using trypan blue exclusion. Cell suspensions were mixed with trypan blue (0.4% [wt/vol]) at a 1:1 volumetric ratio and analyzed with a Luna automated cell counter (Logos Biosystems).

Statistical analysis. All values are presented as means ± standard errors of at least three separate trials. Means of treated groups were compared against those of the appropriate control, and statistical analyses were performed using GraphPad Prism 9 (v9.0.0; San Diego, CA, USA) with Student's *t* test. *P* values of less than 0.05 were considered statistically significant. *P* values of less than 0.01 or 0.001 were considered highly statistically significant.

Ethics statement. Whole blood was donated by a healthy adult volunteer, who provided oral consent, at Clemson University. The collection was approved by Clemson's Institutional Biosafety Committee under safety protocol no. IBC2018-12.

SUPPLEMENTAL MATERIAL

Supplemental material is available online only.

FIG S1, TIF file, 0.9 MB.

FIG S2, TIF file, 0.5 MB.

FIG S3, TIF file, 0.5 MB.

TABLE S1, DOCX file, 0.14 MB.

TABLE S2, DOCX file, 0.01 MB.

ACKNOWLEDGMENTS

This work was funded by National Institute of Allergy and Infectious Disease Grants: AI108287 (WJS, LAT) and AI107950 (LAT) and a National Institute of General Medical Sciences Grant: GM10904 (LAT). The funders had no role in the study design, data collection and analysis, decision to publish, or preparation of the manuscript.

We thank William Marcotte (Department of Genetics and Biochemistry, Clemson University) for the pYES-NT/C plasmid. We thank Ronald Wek (Indiana University School of Medicine) for the pYES2 plasmids containing active or inactive human PKR kinase domains. We thank Lukasz Kozubowski, Mufida Ammar, and Rodney Colon-Reyes (Department of Genetics and Biochemistry, Clemson University) for their kind assistance with culturing yeast strains. We thank Michael Sehorn (Department of Genetics and Biochemistry, Clemson University) for anti-polyhistidine antibody. We thank Thomas Dever (National Institute of Child Health and Development, National Institutes of Health) for custom anti-total yeast eIF2α antibodies and Upinder Singh (Stanford University) for the trigger plasmid. We thank Rooksana Noorai (Clemson University Genomics and Bioinformatics Facility) for helpful discussions on bioinformatic analysis of eIF2α kinases.

REFERENCES

1. Shirley DT, Farr L, Watanabe K, Moonah S. 2018. A review of the global burden, new diagnostics, and current therapeutics for amebiasis. Open Forum Infect Dis 5:ofy161. https://doi.org/10.1093/ofid/ofy161.
2. Grebmer K, Bernstein J, de Waal A, Prasai N, Yin S, Yohannes Y. 2015. Progress on sanitation and drinking water—2015 Update and MDG Assessment. WHO and UNICEF, New York, NY.
3. Bercu T, Petri W, Behm JW. 2007. Amebic colitis: new insights into pathogenesis and treatment. Curr Gastroenterol Rep 9:429–433. https://doi.org/10.1007/s11894-007-0054-8.
4. Hendrick H, Welter BH, Hapstack MA, Sykes SE, Sullivan WJ, Jr, Temesvari LA. 2016. Phosphorylation of eukaryotic initiation factor-2 alpha during stress and encystation in *Entamoeba* Species. PLoS Pathog 12:e1006085. https://doi.org/10.1371/journal.ppat.1006085.
5. Walters HA, Welter BH, Sullivan WJ, Jr, Temesvari LA. 2019. Phosphorylation of eukaryotic initiation factor-2α in response to endoplasmic reticulum and nitrosative stress in the human protozoan parasite, *Entamoeba histolytica*. Mol Biochem Parasitol 234:111223. https://doi.org/10.1016/j.molbiopara.2019.111223.
6. Avron B, Stolarsky T, Chayen A, Mirelman D. 1986. Encystation of *Entamoeba invadens* IP-1 is induced by lowering the osmotic pressure and depletion of nutrients from the medium. J Protozool 33:522–525. https://doi.org/10.1111/j.1550-7408.1986.tb05655.x.
7. Coppi A, Eichinger D. 1999. Regulation of *Entamoeba invadens* encystation and gene expression with galactose and N-acetylglucosamine. Mol Biochem Parasitol 102:67–77. https://doi.org/10.1016/S0166-6851(99)00085-7.
8. Ehrenkaufer GM, Weedall GD, Williams D, Lorenzi HA, Caler E, Hall N, Singh U. 2013. The genome and transcriptome of the enteric parasite *Entamoeba invadens*, a model for encystation. Genome Biol 14:R77. https://doi.org/10.1186/gb-2013-14-7-r77.
9. Field J, Dellen KV, Ghosh SK, Samuelson J. 2000. Responses of *Entamoeba invadens* to heat shock and encystation are related. J Eukaryot Microbiol 47:511–514. https://doi.org/10.1111/j.1550-7408.2000.tb00083.x.
10. Varghese SS, Ghosh SK. 2020. Stress-responsive *Entamoeba* topoisomerase II: a potential antiamoebic target. FEBS Lett 594:1005–1020. https://doi.org/10.1002/1873-3468.13677.
11. Vonlaufen N, Kanzok SM, Wek RC, Sullivan WJ, Jr. 2008. Stress response pathways in protozoan parasites. Cell Microbiol 10:2387–2399. https://doi.org/10.1111/j.1462-5822.2008.01210.x.

12. Dever TE. 1997. Using GCN4 as a reporter of eIF2α phosphorylation and translational regulation in yeast. Methods 11:403–417. https://doi.org/10.1006/meth.1996.0437.
13. Sullivan WJ, Jr, Narasimhan J, Bhatti MM, Wek RC. 2004. Parasite-specific eIF2 (eukaryotic initiation factor-2) kinase required for stress-induced translation control. Biochem J 380:523–531. https://doi.org/10.1042/BJ20040262.
14. Suresh S, Ehrenkaufer G, Zhang H, Singh U. 2016. Development of RNA interference trigger-mediated gene silencing in *Entamoeba invadens*. Infect Immun 84:964–975. https://doi.org/10.1128/IAI.01161-15.
15. Donnelly N, Gorman AM, Gupta S, Samali A. 2013. The eIF2α kinases: their structures and functions. Cell Mol Life Sci 70:3493–3511. https://doi.org/10.1007/s00018-012-1252-6.
16. Vattem K, Staschke KA, Wek RC. 2001. Mechanism of activation of the double-stranded-RNA-dependent kinase, PKR: role of dimerization and cellular localization in the stimulation of PKR phosphorylation of eukaryotic initiation factor-2α (eIF2α). Eur J Biochem 268:3674–3684. https://doi.org/10.1046/j.1432-1327.2001.02273.x.
17. Gietz R, Schiestl RH. 2007. High-efficiency yeast transformation using the LiAc/SS carrier DNA/PEG method. Nat Protoc 2:31–34. https://doi.org/10.1038/nprot.2007.13.
18. Hanks SK, Hunter T. 1995. Protein kinases 6. The eukaryotic protein kinase superfamily: kinase (catalytic) domain structure and classification. FASEB J 9:576–596. https://doi.org/10.1096/fasebj.9.8.7768349.
19. Welter BH, Sehorn MG, Temesvari LA. 2017. Flow cytometric characterization of encystation in *Entamoeba invadens*. Mol Biochem Parasitol 218:23–27. https://doi.org/10.1016/j.molbiopara.2017.10.002.
20. King AV, Welter BH, Koushik AB, Gordon LN, Temesvari LA. 2012. A genome-wide over-expression screen identifies genes involved in phagocytosis in the human protozoan parasite, *Entamoeba histolytica*. PLoS One 7:e43025. https://doi.org/10.1371/journal.pone.0043025.
21. Powell RR, Welter BH, Hwu R, Bowersox B, Attaway C, Temesvari LA. 2006. *Entamoeba histolytica*: FYVE-finger domains, phosphatidylinositol 3-phosphate biosensors, associate with phagosomes but not fluid filled endosomes. Exp Parasitol 112:221–231. https://doi.org/10.1016/j.exppara.2005.11.013.
22. Rao SJ, Meleppattu S, Pal JK. 2016. A GCN2-like eIF2α kinase (LdeK1) of *Leishmania donovani* and its possible role in stress response. PLoS One 11:e0156032. https://doi.org/10.1371/journal.pone.0156032.
23. Zhang M, Mishra S, Sakthivel R, Rojas M, Ranjan R, Sullivan WJ, Fontoura BMA, Ménard R, Dever TE, Nussenzweig V, Jr. 2012. PK4, a eukaryotic initiation factor 2α (eIF2α) kinase, is essential for the development of the erythrocytic cycle of *Plasmodium*. Proc Natl Acad Sci U S A 109:3956–3961. https://doi.org/10.1073/pnas.1121567109.
24. Moraes MC, Jesus TC, Hashimoto NN, Dey M, Schwartz KJ, Alves VS, Avila CC, Bangs JD, Dever TE, Schenkman S, Castilho BA. 2007. Novel membrane-bound eIF2α kinase in the flagellar pocket of *Trypanosoma brucei*. Eukaryot Cell 6:1979–1991. https://doi.org/10.1128/EC.00249-07.
25. Augusto L, Martynowicz J, Amin PH, Carlson KR, Wek RC, Sullivan WJ, Jr. 2021. Tgif2k-B is an eIF2α kinase in *Toxoplasma gondii* that responds to oxidative stress and optimizes pathogenicity. mBio 12:e03160-20. https://doi.org/10.1128/mBio.03160-20.
26. da Silva Augusto L, Moretti NS, Ramos TCP, de Jesus TCL, Zhang M, Castilho BA, Schenkman S. 2015. A membrane-bound eIF2 alpha kinase located in endosomes is regulated by heme and controls differentiation and ROS Levels in *Trypanosoma cruzi*. PLoS Pathog 11:e1004618 https://doi.org/10.1371/journal.ppat.1004618.
27. Holmes MJ, Shah P, Wek RC, Sullivan WJ, Jr. 2019. Simultaneous ribosome profiling of human host cells infected with *Toxoplasma gondii*. mSphere 4:e00292-19. https://doi.org/10.1128/mSphere.00292-19.
28. Tonelli RR, da Silva Augusto L, Castilho BA, Schenkman S. 2011. Protein synthesis attenuation by phosphorylation of eIF2α is required for the differentiation of *Trypanosoma cruzi* into infective forms. PLoS One 6:e27904. https://doi.org/10.1371/journal.pone.0027904.
29. Narasimhan J, Joyce BR, Naguleswaran A, Smith AT, Livingston MR, Dixon SE, Coppens I, Wek RC, Sullivan WJ, Jr. 2008. Translation regulation by eukaryotic initiation factor-2 kinases in the development of latent cysts in *Toxoplasma gondii*. J Biol Chem 283:16591–16601. https://doi.org/10.1074/jbc.M800681200.
30. Pineda E, Perdomo D. 2017. *Entamoeba histolytica* under oxidative stress: What countermeasure mechanisms are in place? Cells 6:44. https://doi.org/10.3390/cells6040044.
31. Rajesh K, Krishnamoorthy J, Kazimierczak U, Tenkerian C, Papadakis AI, Wang S, Huang S, Koromilas AE. 2015. Phosphorylation of the translation initiation factor eIF2α at serine 51 determines the cell fate decisions of Akt in response to oxidative stress. Cell Death Dis 6:e1591. https://doi.org/10.1038/cddis.2014.554.
32. Wek RC, Cavener DR. 2007. Translational control and the unfolded protein response. Antioxid Redox Signal 9:2357–2371. https://doi.org/10.1089/ars.2007.1764.
33. Kim MJ, Kim MN, Min SH, Ham DS, Kim JW, Yoon KH, Park KS, Jung HS. 2019. Specific PERK inhibitors enhanced glucose-stimulated insulin secretion in a mouse model of type 2 diabetes. Metabolism 97:87–91. https://doi.org/10.1016/j.metabol.2018.12.007.
34. Axten JM, Romeril SP, Shu A, Ralph J, Medina JR, Feng Y, Li WH, Grant SW, Heerding DA, Minthorn E, Mencken T, Gaul N, Goetz A, Stanley T, Hassell AM, Gampe RT, Atkins C, Kumar R. 2013. Discovery of GSK2656157: an optimized PERK inhibitor selected for preclinical development. ACS Med Chem Lett 4:964–968. https://doi.org/10.1021/ml400228e.
35. Rozpędek W, Pytel D, Popławski T, Walczak A, Gradzik K, Wawrzynkiewicz A, Wojtczak R, Mucha B, Diehl JA, Majsterek I. 2019. Inhibition of the PERK-dependent unfolded protein response signaling pathway involved in the pathogenesis of Alzheimer's disease. Curr Alzheimer Res 16:209–218. https://doi.org/10.2174/1567205016666190228121157.
36. Zhang M, Gallego-Delgado J, Fernandez-Arias C, Waters NC, Rodriguez A, Tsuji M, Wek RC, Nussenzweig V, Sullivan WJ, Jr. 2017. Inhibiting the *Plasmodium* eIF2α kinase PK4 prevents artemisinin-induced latency. Cell Host Microbe 22:766–776.e4. https://doi.org/10.1016/j.chom.2017.11.005.
37. Augusto L, Martynowic J, Staschk K, Wek RC, Sullivan WJ, Jr. 2018. Effects of PERK eIF2α kinase inhibitor against *Toxoplasma gondii*. Antimicrob Agents Chemother 62:e01442-18. https://doi.org/10.1128/AAC.01442-18.
38. Dias-Teixeira KL, Calegari-Silva TC, Medina JM, Vivarini ÁC, Cavalcanti Á, Teteo N, Santana AKM, Real F, Gomes CM, Pereira RMS, Fasel N, Silva JS, Aktas BH, Lopes UG. 2017. Emerging role for the PERK/eIF2α/ATF4 in human cutaneous leishmaniasis. Sci Rep 7:17074. https://doi.org/10.1038/s41598-017-17252-x.
39. Bateman A, Martin M-J, Orchard S, Magrane M, Agivetova R, Ahmad S, Alpi E, Bowler-Barnett EH, Britto R, Bursteinas B, Bye-A-Jee H, Coetzee R, Cukura A, Da Silva A, Denny P, Dogan T, Ebenezer TGod, Fan J, Castro LG, Garmiri P, Georghiou G, Gonzales L, Hatton-Ellis E, Hussein A, Ignatchenko A, Insana G, Ishtiaq R, Jokinen P, Joshi V, Jyothi D, Lock A, Lopez R, Luciani A, Luo J, Lussi Y, MacDougall A, Madeira F, Mahmoudy M, Menchi M, Mishra A, Moulang K, Nightingale A, Oliveira CS, Pundir S, Qi G, Raj S, Rice D, Lopez MR, Saidi R, Sampson J, The UniProt Consortium, et al. 2021. UniProt: the universal protein knowledgebase in 2021. Nucleic Acids Res 49:D480–D489. https://doi.org/10.1093/nar/gkaa1100.
40. Hulo N, Bairoch A, Bulliard V, Cerutti L, De Castro E, Langendijk-Genevaux PS, Pagni M, Sigrist CJ. 2006. The PROSITE database. Nucleic Acids Res 34:D227–D230. https://doi.org/10.1093/nar/gkj063.
41. Waterhouse AM, Procter JB, Martin DMA, Clamp M, Barton GJ. 2009. Jalview version 2—a multiple sequence alignment editor and analysis workbench. Bioinformatics 25:1189–1191. https://doi.org/10.1093/bioinformatics/btp033.
42. Dereeper A, Guignon V, Blanc G, Audic S, Buffet S, Chevenet F, Dufayard JF, Guindon S, Lefort V, Lescot M, Claverie JM, Gascuel O. 2008. Phylogeny.fr: robust phylogenetic analysis for the non-specialist. Nucleic Acids Res 36:W465–W469. https://doi.org/10.1093/nar/gkn180.
43. Letunic I, Bork P. 2019. Interactive Tree of Life (iTOL) v4: recent updates and new developments. Nucleic Acids Res 47:W256–W259. https://doi.org/10.1093/nar/gkz239.
44. Singh N, Ojha S, Bhattacharya A, Bhattacharya S. 2012. Stable transfection and continuous expression of heterologous genes in *Entamoeba invadens*. Mol Biochem Parasitol 184:9–12. https://doi.org/10.1016/j.molbiopara.2012.02.012.
45. Zhang T, Lei J, Yang H, Xu K, Wang R, Zhang Z. 2011. An improved method for whole protein extraction from yeast Saccharomyces cerevisiae. Yeast 28:795–798. https://doi.org/10.1002/yea.1905.